Journal of Power Sources Advances 36 (2025) 100190

Contents lists available at ScienceDirect

Journal of Power Sources Advances

journal homepage: www.sciencedirect.com/journal/journal-of-power-sources-advances

Analyzing material and production costs for lithium-ion and sodium-ion batteries using process-based cost modeling - CellEst 3.0

Janik Ruppert [a,b,*], Philipp Voß [b,c], Lukas Ihlbrock [b], Jakob Palm [c], Simon Lux [b,c], Jens Leker [a,b]

[a] Helmholtz-Institute Münster (HIMS), Corrensstraße 48, 48149, Münster, Germany
[b] Institute of Business Administration at the Department of Chemistry and Pharmacy (IfbM), University of Münster, Leonardo-Campus 1, 48149, Münster, Germany
[c] Fraunhofer-Einrichtung Forschungsfertigung Batteriezelle FFB, Bergiusstraße 8, 48165, Münster, Germany

ARTICLE INFO

Keywords:
Lithium-ion battery
Sodium-ion battery
Battery cost
Process-based cost modeling

ABSTRACT

In the face of rising demand for efficient and reliable energy storage, this study evaluates the cost-effectiveness of lithium-ion and sodium-ion batteries across pouch, prismatic, and cylindrical cell formats. Introducing CellEst 3.0, an open-source, Excel-based model offering detailed insights into material and production costs for various battery chemistries and formats, including post-lithium technologies such as sodium-ion batteries (SIBs). Our analysis shows that NMC 811 lithium-ion cells offer the highest energy density but have higher material costs due to expensive cathode active material. In contrast, the affordable LFP cathode active material provides cost advantages over NMC. SIBs, particularly those based on NaNFM 111, are the most cost-effective at $54-$62 per kWh, primarily due to cheaper anode active material and aluminum current collector foils. Prismatic cells are identified as the cost leader, supporting the industry's shift towards this format despite other technological factors. Scenario analysis suggests that SIBs withstand volatile market conditions better due to lower material price dependency. While production cost savings correlate closely with cell energy, cylindrical cells are an exception due to their manufacturing processes. This study underlines the value of detailed cost modeling in battery development and demonstrates the economic potential of sodium-ion batteries in sustainable energy storage.

1. Introduction

The global transition towards sustainable energy solutions is increasing the demand for efficient and reliable energy storage systems. Batteries are pivotal in this transformation, serving as fundamental components in renewable energy integration and electric vehicles (EVs). As countries strive to meet ambitious climate targets and reduce their carbon footprints, adopting electric vehicles has emerged as a crucial strategy. While EV sales are rising, a key factor for widespread market penetration is the cost of electric vehicles, particularly the battery, which today accounts for a 28–40 % of EV cost [1–4]. In this context, battery cost modeling emerges as a critical tool to identify cost drivers and explore potential savings in the value chain.

Lithium-ion batteries (LIBs) are currently state-of-the-art for automotive and stationary energy storage systems. However, the volatility in the cost of LIB cathode active material (CAM) precursors, such as lithium carbonate and lithium hydroxide, has sparked interest in post-lithium battery alternatives. Sodium-ion batteries (SIBs) present a potential low-cost alternative in the near term, primarily due to lower material prices and the drop-in capability with LIB production infrastructure [5]. Therefore, it is important to examine SIB costs to determine if they can economically compete with LIBs and become a viable alternative for EVs and stationary applications. Although lithium-carbonate prices are currently low, there is no guarantee they will remain so in the future [6].

Three different battery cell formats, pouch, prismatic, and cylindrical, are commonly used in EVs, although no single format dominates. For instance, BMW has announced a switch from prismatic cells to cylindrical cells in its "*new class*", while VW plans to transition to prismatic cells as part of its "*unified cell*" [7,8]. These strategic decisions raise the question of whether they are cost driven or influenced by other factors, and how they differ across lithium and post-lithium technologies.

Existing cost models and literature do not address this question comprehensively. Many models, such as BatPaC (battery performance and cost model), focus on single cell formats, as do works by Orangi and Strømman, Duffner et al., and Schünemann [9–12]. Ciez and Whitacre, with Pegel et al., have modified BatPaC for cylindrical cells, while

* Corresponding author. Helmholtz-Institute Münster (HIMS), Corrensstraße 48, 48149, Münster, Germany.
E-mail address: jruppert@uni-muenster.de (J. Ruppert).

https://doi.org/10.1016/j.powera.2025.100190
Received 11 August 2025; Received in revised form 19 September 2025; Accepted 5 October 2025
Available online 10 October 2025

Lechner et al. developed a model that compares prismatic and cylindrical cells, thereby including multiple formats [13–15]. Cattani et al. and Börner developed models that allow a comparison of all three cell formats [16,17]. While SIB modeling exists — some based on BatPaC like Vaalma et al., Roberts and Kendrick, Peters et al., and Yao et al. and some as stand-alone calculations like Berg et al. — these models do not allow for comparison across cell formats (see S1 Supporting Information Table A3 for full comparison) [18–22].

The process-based material and production cost model *CellEst 3.0* is introduced here to compare the costs of LIBs and SIBs across all major cell formats. Building upon the material cost model *CellEst 2.0*, published in 2021 [23], *CellEst 3.0* is a highly transparent, Excel-based, open-source, and process-based model enabling comparisons of LIBs, SIBs, and different cell formats. All calculations and input data are specified to ensure reproducibility, including current primary energy data from the research battery factory Fraunhofer FFB in Münster. Furthermore, the model is employed to investigate whether decisions for specific cell formats are cost-driven and sustainable concerning post-lithium batteries.

2. Methods

2.1. Model architecture

CellEst 3.0 uses a bottom-up process-based cost modeling approach, which was first introduced by Field, Kirchain and Roth (2007) but has since been widely used for battery cost modeling [24,25]. This approach can be used to analyze the influence of individual technology and cost parameters and the cost structure of production at a high level of granularity, distinguishing costs for each material and process step. The material and production cost model developed here for large-scale battery production is published open-source as an Excel-model to ensure maximum transparency and flexibility (see E1 CellEst 3.0 Model). It can thus serve as a basis for researchers, companies or decision makers to modify and use the model for their own needs. All input parameters are adjustable, thus enabling cost hotspot analysis and facilitating strategic decision-making. The developed model CellEst 3.0 comprises three interconnected sub-models: the cell model and the process model, which are then integrated into the cost model (cf. Fig. 1).

2.1.1. Cell model

The cell model creates a virtual battery cell based on geometric constraints and material data, calculating among others the cell's capacity and energy, and a bill of materials (BOM; see supporting information S2 model manual for more details). The calculation logic in this sub-model is partially based on the two previous iterations of *CellEst*: *CellEst 1.0* by Wentker, Greenwood, and Leker (2019) and *CellEst 2.0* by Greenwood, Wentker, and Leker (2021) [23,26]. However, it has been expanded to include prismatic and cylindrical cells accounting for their geometric characteristics and now includes over 100 variable input parameters. Further, post-lithium technologies can be modeled, and the volume change of the cathode and anode is calculated more accurately by including irreversible volume changes, as well as reversible crystal volume changes during cycling. This means that many different cell geometries and compositions can be analyzed with the model, allowing versatile use and, in particular, quick and easy cost estimation for academic, but also industrial scale analyses.

In the cell model, the internal dimensions are derived from external geometry. The thickness of the cathodes and anode coating is then determined through a case differentiation considering the N/P capacity ratio and volume changes [23]. Up to this point, the calculations for pouch and prismatic cells, which consist of stacked cell stacks, are similar to those for cylindrical cells, which contain a wound jelly roll. For pouch and prismatic cells, the number of cell stacks that fit within the cell is determined, whereas for cylindrical cells, the lengths of the wound cathode and anode are calculated. Based on this, the cell's capacity and energy are determined using either the number of cell stacks or the cathode length. Next, the mass of all active and inactive components is calculated to generate the cell's BOM and to calculate energy densities.

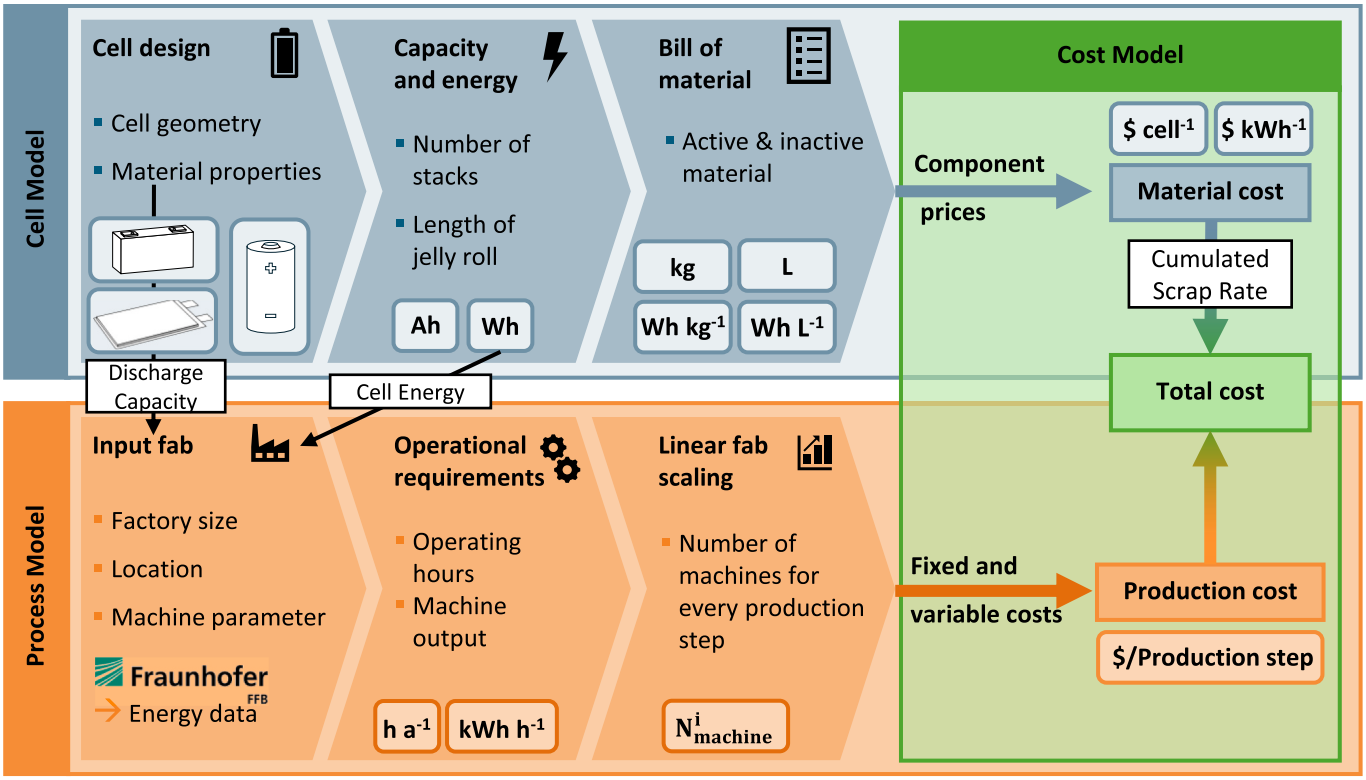

Fig. 1. The general model architecture of CellEst 3.0 with model outputs shown in the round boxes.

2.1.2. Process model

The process model simulates a large-scale battery factory, based on user-defined specifications for factory size, location and technical machine parameters. It requires input from the cell model, including the active material's capacity and energy per cell. For the energy demand of the machines, primary industry data provided by the Fraunhofer FFB Fab are used and published [27]. In addition, the model includes further operating parameters (see Table 2) such as working days and shifts per day, so that this sub-model includes a total of 250 variable input parameters. The integer number of machines per production step scales linearly with the predefined factory output in GWh. However, one of these production steps acts as a bottleneck, requiring the factory output to be adjusted accordingly.

2.1.3. Cost model

Material costs are quantified per cell and per kWh using component prices, primarily in USD kg^{-1}. They are adjusted for the reversed cumulative scrap rate, which is higher the earlier a material enters the production process. Production costs, consisting of capital cost for investments, energy, labor, building, dry room, and overhead, are subsequently calculated for each production step. The total costs result from the material costs and the sum of all fixed and variable production costs, expressed in USD kWh^{-1} for each process step (cf. equation (1)).

$$C_{Total} = \sum_{i}^{n} C_{Material,i} + \sum_{j}^{n} \left(C_{Invest,j} + C_{Energy,j} + C_{Labor,j} + C_{Building,j} + C_{DryRoom,j} + C_{Overhead,j} \right) \quad (1)$$

2.2. Parameterization of the analysis

For this comparison and to showcase the model, two LIBs were modeled: an $LiNi_{0.8}Mn_{0.1}Co_{0.1}O_2$ (NMC 811) based battery, chosen for its high discharge capacity of 200 mAh g^{-1} (Table 1), making it suitable for automotive applications requiring high energy density; and an $LiFePO_4$ (LFP) based battery, selected as a lower-cost option at 150 mAh g^{-1} with potential benefits for affordable electric vehicles. This selection reflects the current EV market where approximately 55 % of batteries are nickel rich NMC- and 40 % LFP-based LIBs [28]. Graphite is the state-of-the-art anode active material (AAM) and modeled in both cell designs. For simplicity, the cells are addressed only with the name of the CAM in the following.

Sodium, the second alkali metal after lithium, allows SIBs to utilize similar active material structures. Literature identifies promising SIB CAMs including single and multiple transition metal layered oxides like $NaMnO_2$ and $NaNi_{1/3}Fe_{1/3}Mn_{1/3}O_2$ (NaNFM111), polyanionic compounds, and Prussian blue analogues [31,32]. The O3-type multi-metal layered oxide NaNFM 111, containing nickel, iron and manganese, is highlighted for its electrochemical performance at 160 mAh g^{-1} and the representation of recent trends in commercialization according to Yao et al. [21] The polyanionic NFPP ($Na_4Fe_3(PO_4)_2(P_2O_7)$) serves as the sodium counterpart to LFP, showing lower performance but also lower cost, justifying its inclusion in this analysis.

Graphite is typically replaced by amorphous hard carbon (HC) for the SIB AAM due to the thermodynamic instability of binary Na^+/graphite intercalation compounds. Additionally, the anode current collector foil (ACCF) of SIBs advantageously is based on aluminum instead of copper because sodium does not alloy with aluminum at low potentials [19,20].

Cost calculations in *CellEst 3.0* rely on current spot prices, sourced from up-to-date market reports and the information platform Shanghai Metal Market (cf. Table 1), to reflect recent price dynamics. This paper offers a cost comparison across the three cell formats in electromobility — pouch, prismatic and cylindrical, taking into account constraints such as the large format preference and height limitations for underbody installation in EVs [33].

Three cell formats were selected (Table 2) based on Neef et al. (2022) [33]. Pouch and prismatic cells are assumed to use stacked electrode configurations with Z-folding, while cylindrical cells employ a wound jelly roll, leading to variations in production processes during assembly. The input parameters for modeling a hypothetical battery cell factory, including operation, cost factors, cost modeling, and p-values for economies of scale, are detailed in Table 2. In the model, China was selected as the production location, which affects cost factors like energy, labor, and building.

Table 2
General input parameter for format and production.

Parameter	Value	Unit	Reference
Pouch (Hight x Width x Thickness)	330x162x7	mm	
Prismatic (Width x Hight x Thickness)	300x100x30	mm	
Cylindrical (Diameter x Height)	46x80	mm	
Annual Capacity	5	GWh a^{-1}	
Production Location	China		
Working Days per Year	360	d	[10]
Shifts per day	3		[10]
Hours per shift	8	h	[10]
Paid Breaks	1	h	[10]
Labor Cost	5.5	USD h^{-1}	[34]
Energy Cost (electric)	0.09	USD kWh^{-1}	[35]
Energy Cost (gas)	0.058	USD kWh^{-1}	[36]
Area Cost	581	USD m^{-2}	[37]
Discount Rate	8	%	[15]
Overhead Rate	35	%	[38]
Maintenance Rate	10	%	[13]
Unplanned Downtime	25	%	[15]
Building Area Multiplier	440	%	[10]
Lifetime Machines	10	a	[9]
Lifetime Buildings	20	a	[9]
Investment P-Value	0.9		[39]
Energy P-Value	0.95		[39]
Labor P-Value	0.7		[39]
Area P-Value	0.95		[39]

3. Results and discussion

3.1. Comparative analysis of cell energy and energy densities

The gravimetric and volumetric energy densities (in Wh kg^{-1} and Wh L^{-1}) of NMC 811 are the highest as NMC 811 is the analyzed CAM with the highest theoretical discharge capacity consistent with existing

Table 1
Applied active material parameters and costs which serve as input parameters for the cell model.

Parameter	Unit	NMC 811	LFP	NaNFM 111	NFPP	Graphite	Hard Carbon
Practical Discharge Capacity	mAh g^{-1}	200	150	160	128	360	325
Discharge Potential	V	3.7	3.3	3.3	3.1	0.1	0.2
Density	g cm^{-3}	4.78	3.45	4.52	3.2	2.25	1.5
Material Cost	USD kg^{-1}	22.6 [29] [a]	6.0 [30]	7.3 [29] [b]	4.13 [29] [c]	7.5 [30]	5.2 [29] [b]

[a] Retrieved in May 2024.
[b] Retrieved in September 2024.
[c] Retrieved in April 2025.

literature (see Fig. 2) [40]. The energy densities of LFP and NaNFM are at similar levels, while NFPP shows slightly lower values. The volumetric energy density seems to depend mainly on cell chemistry, whereas for the gravimetric energy density a trend is observable between cell formats. Pouch cells have the highest gravimetric energy density because they consist of lightweight polymer-aluminum composite foils instead of nickel-plated steel for cylindrical or aluminum for prismatic cells. However, these observations are only at the cell level and could be offset at the pack level, for example through cell-to-pack approaches [21]. Prismatic cells follow as they are significantly larger than cylindrical 4680 cells, favoring the active/inactive material ratio. For the CAMs, a similar distribution can be observed regarding cell energy. The NMC 811 cells have the highest cell energy, mainly due to the high active material capacity and high operating voltage, whereas NFPP has the lowest cell energy due to the lower material performance (see S1 Supporting Information, Fig. A1 for a parameter dependency heat map). Meanwhile, the cell energy of NaNFM is slightly lower (15–17 %) compared to LFP, although the CAM capacity is 14 % higher (in mAh g^{-1}, see Table 1). This is primarily due to the limitations of the HC used as AAM. The model first defines the maximum thickness of the electrode coating (set at 100 µm) and then calculates whether the cathode or anode can match the maximum thickness so that the N/P ratio between the anode and cathode is maintained. Thus, while the cathode thickness is maximized for the LFP cells, the cathode thickness for NaNFM is only 68 µm due to the capacity and voltage limitations of the HC.

The cylindrical cells have the lowest cell energy with 32–75 Wh, followed by the pouch cells (79–184 Wh), and the prismatic cells (235–547 Wh). The trend can be explained by the differing cell dimensions and sizes, which determine the amount of active materials inside the cell. Thus, the cylindrical cells only contain 97–115 g CAM, while the prismatic cells contain 723–851 g CAM. This distinction is important because there is a direct correlation between cell energy and production cost, as more cylindrical cells have to be produced to achieve the same battery capacity in GWh per year, which increases production costs on the cell level.

3.2. Comprehensive cost analysis

When assessing total costs, NMC 811 emerges as the most expensive option, while LFP is 17–19 % cheaper (see Fig. 3). NaNFM is the most cost-effective, offering a 0.4–3 % cost reduction compared to LFP. NFPP performs worse than NaNFM due to its lower capacity and working potential, and is on a par with LFP, depending on the cell format. Additionally, cost differences between cell formats are evident, with similar trends observed across all cell chemistries. Pouch cells are the most expensive regardless of cell chemistry, whereas cylindrical cells are cheaper by 5–11 %. Prismatic cells are slightly cheaper than cylindrical cells, with a cost difference of 2–4 %.

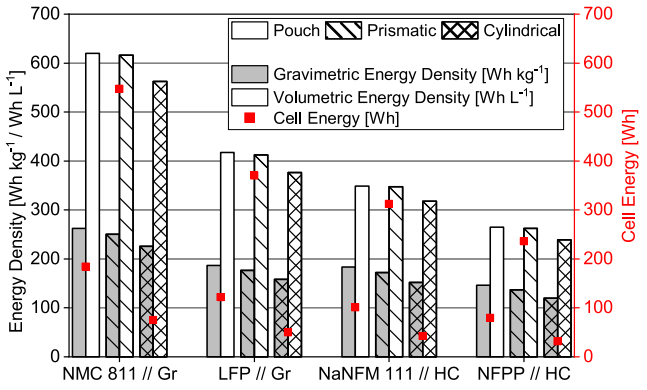

Fig. 2. Gravimetric and volumetric energy densities (left, in Wh kg^{-1} and Wh L^{-1}) and cell energy of the modeled battery cells (right, in Wh).

The elevated costs of NMC 811 cells mainly stem from the CAM, which accounts for 54–59 % of the total costs, compared to 26–29 % for LFP, 32–36 % for NaNFM, and 23–26 % for NFPP cells. NMC enables the highest energy density (see Table 1), but its cost per kg is three to five times higher than the other materials due to its expensive metal precursors, containing nickel and cobalt. Therefore, NMC cells would be most affected by volatile market prices for these metal precursors.

However, NMC cells are the cheapest to produce at \$9–14 kWh^{-1}. The production costs of LFP cells are higher, ranging from \$14 to \$19 per kWh, with the cost of inactive materials and AAM also being elevated. The latter is due to the lower cell energy of LFP cells, as more cells and therefore more inactive materials and AAM are required to produce the same kWh of battery. Nevertheless, this is completely offset by the much lower CAM cost, resulting in a lower overall cost of the LFP cell.

NaNFM cells are the most cost effective despite their higher production cost of \$15–22 kWh^{-1}. Additionally, the CAM is slightly more expensive, despite substituting lithium with cheaper sodium. Sodium salt ($NaPF_6$) can be used as the conducting salt in the electrolyte for SIBs [20]. However, the resulting cost advantage is only marginal (see S2 Model Manual for further information). The primary factors contributing to the cost advantage of SIBs are AAM and ACCF.

HC as AAM results in a cost reduction of \$1.80 kWh^{-1} compared to graphite in LFP cells, despite its lower capacity and density. Here, the lower volume change of HC (4 %, compared to 13.4 % for Gr) has only a minor impact, with the main reason for the cost advantage being the lower material cost (see Table 1 and S1 Supporting Information Figure A1). Using aluminum as the ACCF reduces the cost by ~\$6 kWh^{-1} and improves gravimetric energy density due to its lower density, making aluminum ACCF a key advantage of SIBs. However, these results are highly dependent on the assumptions made for capacity and voltage, and it is not yet certain that these can be achieved in practice [21]. These advantages also apply to NFPP and, together with the low-cost CAM, results in the lowest material cost of all examined cells. However, the low cell energy leads to the highest production costs of \$20–27 kWh^{-1}, which completely negates this advantage. This is especially apparent for NFPP pouch cells where production makes up 34–41 % of total cost, putting them on par with LFP.

When examining cell formats, it is evident that lower cell energy results in higher production costs. This is also evident across cell chemistries, where cell energy drops by 43 % from NMC 811 to NFPP, while production costs increase by 90–117 %, and in pouch and prismatic cells, both of which use Z-folding. As cell energy decreases, more cells need to be processed to achieve the factory output, requiring more machines, energy and labor, thus increasing costs.

The only exception are cylindrical cells, which have the lowest cell energy but also production costs that are below pouch cells and only slightly above prismatic cells. This is despite their low cell energy due to geometric differences, resulting in cost savings in the welding process and end-of-life testing (EOL). The production steps involving the processing of full cells are typically the most impacted. For example, one EOL testing machine is required for prismatic NMC cells, while six are required for cylindrical NMC cells, as more cells need to be processed in total. The low production costs are mainly due to the different production processes, as the separation and Z-folding of the electrode stack is replaced by winding of the jelly roll in cylindrical cells. This saves costs by eliminating one production step in the model.

Prismatic cells emerge from the analysis as the most cost-effective. This is due to lower production costs due to high cell energy, slightly lower material costs from lower scrap rates during production (scrap rate for separating and z-folding is lower than for winding) and the slightly lower cost of the packaging container. Prismatic cells are therefore the best cell format from a pure cost point of view. However, the discrepancy is not substantial, and it is debatable whether it will be outweighed by other factors, for example at the battery pack level, such

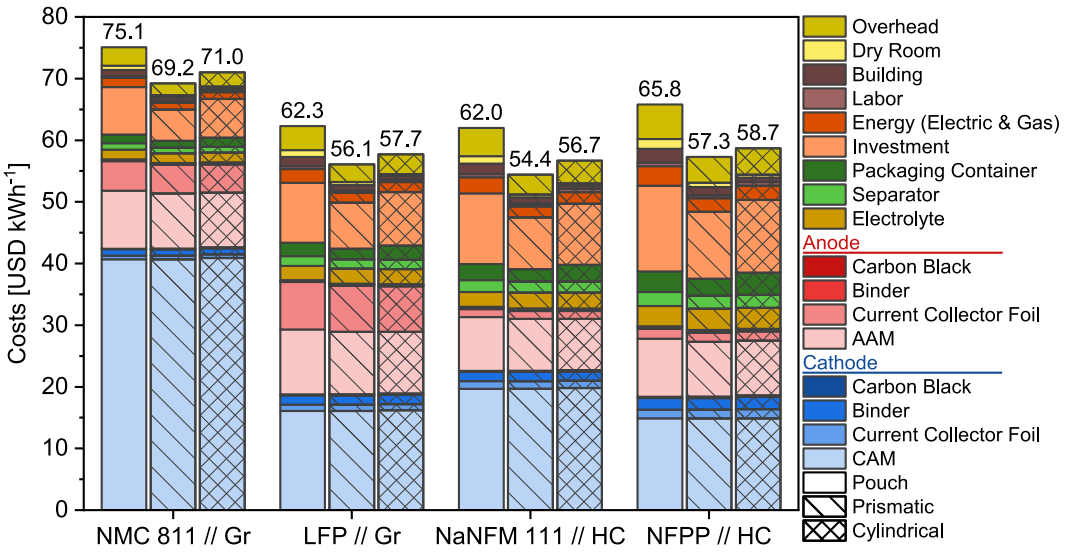

Fig. 3. Comprehensive cost analysis in USD kWh^{-1} of the battery cells examined (see S1 Supporting Information for all data points).

as the trend towards cell-to-pack design [41].

3.3. Scenario analysis

To assess the economic competitiveness of the modeled LIBs and SIBs, three material scenarios were considered: nickel price, sodium and lithium price, as well as scrap rate alongside three production scenarios: discount rate, energy, and labor costs (see Fig. 4). The factors that are selected are most likely to be influenced by external factors such as market volatility, quality issues, interest rates, energy, and wage levels, and are largely beyond a manufacturer's control. A pouch cell was modeled for the material side and an NMC 811 CAM for the production side. Each input factor was adjusted by 50 %, assessing the percentage impact on total cell cost.

For the nickel price scenario, the input price for nickel sulfate shifted from \$3.8 kg^{-1} to \$1.9 kg^{-1} and \$5.7 kg^{-1}. The analysis showed a \$7.4 kWh^{-1} increase in total cost for NMC 811 cells with a 50 % nickel price spike, the highest change among examined scenarios, due to its high nickel content. As the mixed oxide NaNFM 111 is only one third nickel, it was less affected despite requiring more CAM in kg kWh^{-1}, while LFP and NFPP were unaffected due to their lack of nickel.

In the Li/Na scenario, the impact of different input prices for lithium carbonate, lithium hydroxide, and sodium carbonate was analyzed. This consideration is especially relevant due to recent lithium price volatility. LIB costs were more sensitive than SIBs because lithium compounds costs are 20 times higher than sodium carbonate, so a percentage change in lithium price results in a greater absolute change [42,43]. Sodium's small proportion in NaNFM and NFPP CAM cost results in a minor overall impact on total cell cost.

The scrap rate has a significant impact on the total cost, as the

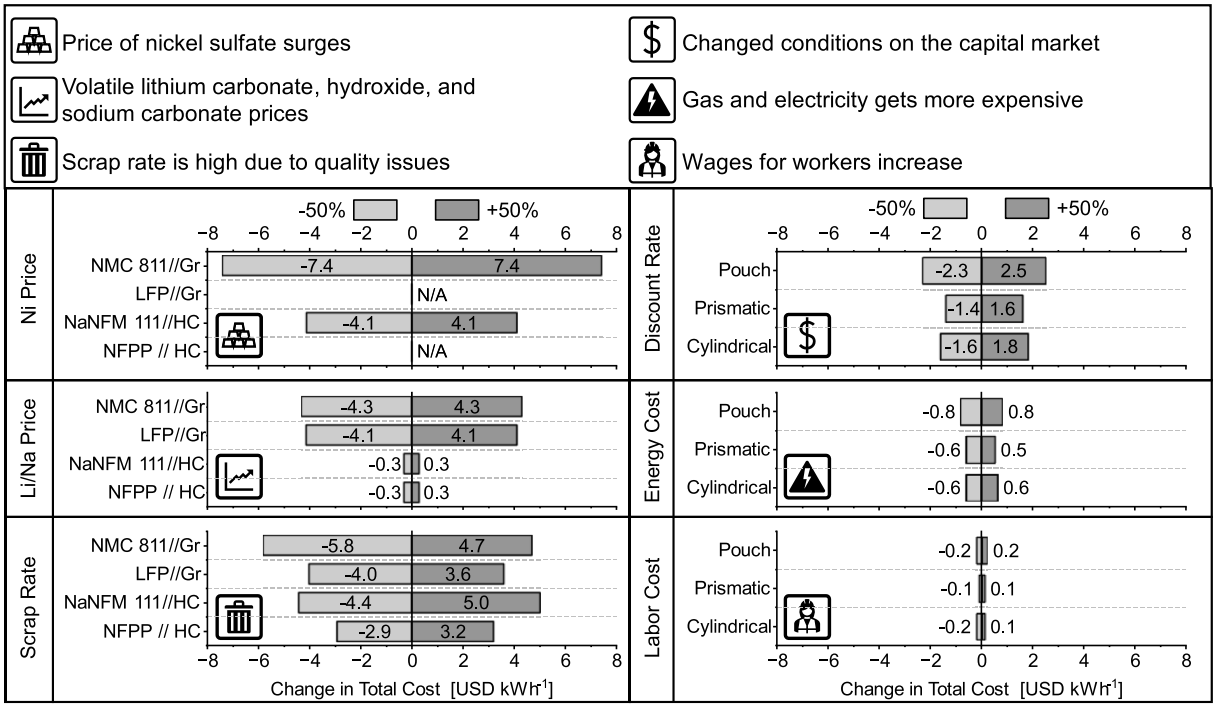

Fig. 4. Results of the scenario analysis as change in total costs.

material costs are the largest share of the total cost. Halving the cumulative scrap rate reduces the cell cost by \$2.9–5.8 kWh^{-1} (5–7 %), with the greatest impact on cells with high material costs. Fig. 4 reveals asymmetrical effects on cost due to the scrap rate's influence on both material cost and production output. A lower scrap rate increases machine output, necessitating fewer machines and thereby reducing costs. However, because only whole numbers of machines can be used, the reduction potential is limited for low scrap rates, as the number of machines cannot be reduced below one machine, which explains the asymmetry. Thus, while the scrap rate is one of the most effective levers for cost reduction, it can also pose challenges if high scrap rates occur during ramp-up or persistent quality issues, as seen at Northvolt, making cost-effective production and especially ramp-up more challenging [44].

Production scenarios reveal less significant impacts. The discount rate influences the capital cost of machinery, buildings, and dry rooms, having the greatest impact at \$1.4–2.5 kWh^{-1} (2–3 %), with its significance declining as production costs decrease for the cell formats. In contrast, energy and labor costs have minimal impact in a Chinese production context where wages and energy costs are low, with an assumed Chinese labor cost of \$5.51 h^{-1}. A 50 % increase raises this to \$8.27 h^{-1}, still well below the German wage level of around \$44 h^{-1} [45]. While this analysis illustrates the variability of Chinese labor costs, it does not provide a location-specific comparison.

The analysis reveals a low dependence on production factors and a significant potential impact from material factors. NaNFM shows higher resilience to nickel metal price increases than NMC and significantly better resilience to lithium/sodium price increases, putting it on par with LFP in terms of the impact of market volatility. NFPP shows the greatest resilience as it does not depend on nickel or lithium. The gap between LIBs and SIBs is largely dependent on the development of metal prices. In line with Yao, Benson and Chueh [21], a rising nickel price would cause the cost advantage of NaNFM to shrink, and a rising lithium/sodium price would cause it to increase. A general increase in metal prices would reduce the disadvantage of NFPP. The Yao, Benson, and Chueh study predicts a SIB cost advantage from 2030 to 2040, depending on market development, whereas the results in this study already indicate a cost advantage at this point in time, presumably due to differences in assumptions.

3.4. Comparison with other work

To contextualize this work, comparing it with other cost models and market studies is crucial for validating the model's accuracy, identifying common trends in the literature, and assessing its ability to reflect current battery costs. Several factors must be considered in these comparisons, such as whether costs are reported at the cell or system level, and the specific chemistry and format being analyzed. It is also important to note how process costs and cost factors are integrated.

Orangi et al. [46] analyze the cost decline of LIBs based on historical data and provide cost trajectories. They report on an LFP cell in 2024 at \$75.1 kWh^{-1} and an NMC 811 cell at \$86.7 kWh^{-1}, although the cell format remains unclear. Thus, the LFP cell of Orangi et al. is 17–25 % more expensive, and the NMC cell is 13–20 % more expensive than the cells modeled in this work. However, the cost disparity between the two chemistries is similar in Orangi et al. (13 %) and this work (13–19 %). A similar relationship between the LIBs is apparent, even though the absolute values differ across papers, which cannot be attributed to a definitive cause due to the diversity of the input parameters.

Pegel et al. [14] model a 4680 cylindrical cell with NMC 811 as CAM using a modification of BatPaC, resulting in a cost of \$96.12 kWh^{-1}. The reasons for the cost disparity compared to this work likely lie in the input parameters for materials, which date from 2018 to 2022 in Pegel et al., where higher prices are assumed for CAM and separators.

Lechner et al. [15] provide an explicit analysis of a prismatic and a 4680 cylindrical cell for NMC 811 and LFP. They report full costs of \$95.5 kWh^{-1} for the prismatic NMC 811 cell and \$96 kWh^{-1} for the cylindrical, with the prismatic LFP cell at \$99.5 kWh^{-1}. Two things can be observed here: first, the reported costs are significantly higher than the modeled costs in this work, and second, the relationship between NMC and LFP is inverse, which is noted but not explained by Lechner et al. The likely reason for both observations is the use of older data before the sharp rise in lithium prices around 2022 [47]. For example, Lechner et al. assume a value of \$9 kWh^{-1} for LFP from a 2020 source, which is 50 % higher than the value in this paper.

Comparing SIBs is more challenging due to fewer publications in this area. Vaalma et al. [19] use BatPaC to calculate the material and production costs of SIB, determining the costs as of 2018 and offering an outlook on potential improvements with further developed materials. By subtracting battery pack and module-related costs, Vaalma et al.'s costs can be determined at the cell level, resulting in \$146 kWh^{-1} for an NMC 622 cell, \$182 kWh^{-1} for LFP, and \$141–184 kWh^{-1} for SIB, depending on the state of development. This leads to a 20 % cost advantage for NMC 622 compared to LFP, contrasting with the 14 % cost advantage for LFP found in this study, which indicates a shift in cost dynamics since the publication by Vaalma et al. Peters et al. developed their own model and analyzed a cylindrical 18650 cell for NMC 111, LFP, and SIB, resulting in costs of \$168.6 kWh^{-1}, \$229.3 kWh^{-1}, and \$223.4 kWh^{-1} for each, respectively [20]. Both studies estimate LFP to be more expensive than NMC, and SIBs to be at a similar level to LFP. According to Vaalma et al., SIBs have the potential to reach costs comparable to NMC batteries. However, all costs from these studies are considerably higher than those in this study, attributed to improved manufacturing processes and cheaper materials due to economies of scale in a rapidly growing energy storage market.

Additionally, current market studies on cell costs can be consulted. BloombergNEF [48] reports a cell cost of \$78 kWh^{-1} for LIBs, and the Intercalation Battery Component Price Report February 2024 [30] lists costs of \$66 kWh^{-1} for NMC cells and \$53 kWh^{-1} for LFP cells. These values are significantly lower than those from the studies considered. Since there is always a time lag between data collection and publication in scientific articles, it can be assumed that cell costs have fallen again in recent years. Differences in assumptions and calculation methods may also explain these results. The results of this work, at \$69–75 kWh^{-1} for NMC cells and \$56–62 kWh^{-1} for LFP, are much closer to current costs from the market reports, underscoring *CellEst 3.0's* relevance in modeling current trends.

4. Conclusion

Our study shows that NMC 811 cells are the most expensive, priced at \$69–75 kWh^{-1} due to their CAM, despite having the lowest production costs. The favorable CAM cost is the biggest advantage for LFP cells summing up to \$56–62 kWh^{-1}, which results in the cost advantage over NMC. NFPP pouch cells cost \$66 kWh^{-1} and are more expensive than LFP, while prismatic and cylindrical NFPP cells are comparable to equivalent LFP cells at \$57 kWh^{-1}. NaNFM 111 based SIB cells show the lowest cost at \$54–62 kWh^{-1} despite their high production cost, with the advantage coming from HC as the AAM and aluminum as the ACCF. These results suggest a small cost advantage of SIBs, although the advantage depends heavily on whether the capacity and voltage of the active materials can be realized in practice on a GWh per year scale.

In terms of production costs, there is a clear trend that higher cell energy leads to lower production costs, although cylindrical cells are an exception due to differences in the production process. When comparing formats, prismatic cells emerge as the cost leader, supporting VW's move towards the prismatic "*unified cell*" [7]. The cost advantage over cylindrical cells is 2–4 % and 8–12 % over pouch cells. This cost advantage must be balanced with technological differences in the cell formats, e.g. in terms of charging behavior, cooling or integration in the vehicle. In addition, these are cell-only costs and do not consider pack-level cost effects, although the latest trend in cell-to-pack designs also favors prismatic cells [33].

The scenario analysis shows that NMC is the least resilient to volatile precursor markets, with LFP and NaNFM roughly on par. While LFP is more affected by changes in lithium and sodium prices, NaNFM is similarly impacted by nickel prices. There is no clear advantage between LFP and NaNFM in terms of resilience. In contrast, NFPP is largely unaffected due to its cheap and abundant precursor materials and can potentially be cost-effective in volatile market conditions. Changes in cost leadership thus heavily depend on individual metal price trends. The scrap rate in specific production steps offers significant cost-saving potential that can be actively influenced. It is comparable to the cost of precursor materials and poses a substantial risk if cells cannot be produced with adequate quality. Total cell costs show low dependency on production factors, although only variations in Chinese production were considered. However, the impact on European production could be significantly higher and could be investigated in future research.

A comparison of the *CellEst 3.0* results with the latest cell cost research and cost modeling shows that *CellEst* cell costs are consistently lower than those of other models. However, *CellEst 3.0* is also much closer to current market studies on cell costs and is therefore better suited to accurately reflect current trends and developments. It is also the only model capable of modeling all relevant cell formats and, at the same time, LIBs and post-lithium batteries with SIBs (as shown in S1 Supporting Information Table A3). As an open-source model, *CellEst 3.0* will provide a platform for other researchers to incorporate their own technologies, thereby broadening the scientific discourse on post-lithium technologies by including a cost analysis.

CRediT authorship contribution statement

Janik Ruppert: Writing – original draft, Visualization, Software, Methodology, Investigation, Formal analysis, Data curation, Conceptualization. **Philipp Voß:** Writing – original draft, Validation, Methodology. **Lukas Ihlbrock:** Writing – original draft, Validation, Methodology. **Jakob Palm:** Writing – original draft, Data curation. **Simon Lux:** Writing – original draft. **Jens Leker:** Writing – original draft, Supervision.

Declaration of competing interest

The authors declare that they have no known competing financial interests or personal relationships that could have appeared to influence the work reported in this paper.

Glossary

EV - Electric vehicle; LIB – Lithium-ion battery; SIB – Sodium-ion battery; CAM – Cathode active material; BatPaC – Battery performance and cost model; BOM – Bill of materials; AAM – Anode active material; NMC – Lithium nickel manganese cobalt oxide; LFP – Lithium iron phosphate; NaNFM – Sodium nickel iron manganese oxide; NFPP - $Na_4Fe_3(PO_4)_2(P_2O_7)$; Gr – Graphite; HC – Hard carbon; ACCF – Anode current collector foil; CCCF – Cathode current collector foil; EOL – End of line testing.

Appendix A. Supplementary data

Supplementary data to this article can be found online at https://doi.org/10.1016/j.powera.2025.100190.

Data availability

Data will be made available on request.

References

[1] European Environment Agency, New data: CO2 emissions from new cars and vans further decrease as electric vehicle sales grow in Europe. https://www.eea.europa.eu/en/newsroom/news/new-data-co2-emissions-of-new-cars-and-vans, 2025. (Accessed 14 April 2025).

[2] C. McKerracher, The EV price gap narrows | BloombergNEF. https://about.bnef.com/blog/the-ev-price-gap-narrows/, 2021. (Accessed 14 April 2025).

[3] A. König, L. Nicoletti, D. Schröder, S. Wolff, A. Waclaw, M. Lienkamp, An overview of parameter and cost for battery electric vehicles, WE! 12 (2021) 21, https://doi.org/10.3390/wevj12010021.

[4] Statista, Battery share of large EV costs 2030| statista. https://www.statista.com/statistics/797638/battery-share-of-large-electric-vehicle-cost/, 2017. (Accessed 15 May 2025).

[5] F. Duffner, N. Kronemeyer, J. Tübke, J. Leker, M. Winter, R. Schmuch, Post-lithium-ion battery cell production and its compatibility with lithium-ion cell production infrastructure, Nat. Energy 6 (2021) 123–134, https://doi.org/10.1038/s41560-020-00748-8.

[6] C. Perry, E. Thomson, Facing the tightening lithium supply challenge in 2025. https://www.fastmarkets.com/insights/facing-the-tightening-lithium-supply-challenge-in-2025/, 2025. (Accessed 6 August 2025).

[7] H. Yang, Volkswagen to Switch EV Battery Type, Leaving Supply Deals in Doubt - Sources, Reuters Media, 2021. (Accessed 14 April 2025).

[8] CATL Says to Supply BMW with Cylindrical Cell from 2025, Reuters Media, 27 May 2022. (Accessed 14 April 2025).

[9] K.W. Knehr, J. Kubal, P.A. Nelson, S. Ahmed, Battery Performance and Cost Modeling for Electric-Drive Vehicles - a Manual for BatBaC v5.0, Argonne National Lab., 2022.

[10] J.-H. Schünemann, Modell Zur Bewertung Der Herstellkosten Von Lithiumionenbatteriezellen, Fakultät für Maschinenbau der Technischen Universität Carolo-Wilhelmina zu Braunschweig, 2015.

[11] S. Orangi, A.H. Stromman, A techno-economic model for benchmarking the production cost of lithium-ion battery cells, Batteries 8 (2022).

[12] F. Duffner, L. Mauler, M. Wentker, J. Leker, M. Winter, Large-scale automotive battery cell manufacturing: analyzing strategic and operational effects on manufacturing costs, Int. J. Prod. Econ. 232 (2021) 107982, https://doi.org/10.1016/j.ijpe.2020.107982.

[13] R.E. Ciez, J.F. Whitacre, Comparison between cylindrical and prismatic lithium-ion cell costs using a process based cost model, J. Power Sources 340 (2017) 273–281, https://doi.org/10.1016/j.jpowsour.2016.11.054.

[14] H. Pegel, A. Grimm, C. Frey, V. Seefeldt, S. Baazouzi, D.U. Sauer, Manufacturing of tabless cylindrical lithium-ion cells: quantifying the influence of cell dimensions and housing material via process-based cost d modeling, J. Energy Storage 98 (2024) 112863, https://doi.org/10.1016/j.est.2024.112863.

[15] M. Lechner, A. Kollenda, K. Bendzuck, J.K. Burmeister, K. Mahin, J. Keilhofer, L. Kemmer, M.J. Blaschke, G. Friedl, R. Daub, A. Kwade, Cost modeling for the GWh-scale production of modern lithium-ion battery cells, Commun. Eng. 3 (2024) 155, https://doi.org/10.1038/s44172-024-00306-0.

[16] N. Soldan Cattani, E. Noronha, J. Schmied, M. Frieges, H. Heimes, A. Kampker, Comparative cost modeling of battery cell formats and chemistries on a large production scale, Batteries 10 (2024) 252, https://doi.org/10.3390/batteries10070252.

[17] M.F. Börner, Ein Prozessbasiertes Modell Zur Berechnung Der Kosten Von Lithium-Ionen-Batteriezellen, RWTH Aachen University, 2024.

[18] S. Roberts, E. Kendrick, The re-emergence of sodium ion batteries: testing, processing, and manufacturability, Nanotechnol. Sci. Appl. 11 (2018) 23–33, https://doi.org/10.2147/NSA.S146365.

[19] C. Vaalma, D. Buchholz, M. Weil, S. Passerini, A cost and resource analysis of sodium-ion batteries, Nat. Rev. Mater. 3 (2018), https://doi.org/10.1038/natrevmats.2018.13.

[20] J. Peters, A. Peña Cruz, M. Weil, Exploring the economic potential of sodium-ion batteries, Batteries 5 (2019) 10, https://doi.org/10.3390/batteries5010010.

[21] A. Yao, S.M. Benson, W.C. Chueh, Critically assessing sodium-ion technology roadmaps and scenarios for techno-economic competitiveness against lithium-ion batteries, Nat. Energy 10 (2025) 404–416, https://doi.org/10.1038/s41560-024-01701-9.

[22] E.J. Berg, C. Villevieille, D. Streich, S. Trabesinger, P. Novák, Rechargeable batteries: grasping for the limits of chemistry, J. Electrochem. Soc. 162 (2015) A2468–A2475, https://doi.org/10.1149/2.0081514jes.

[23] M. Greenwood, M. Wentker, J. Leker, A bottom-up performance and cost assessment of lithium-ion battery pouch cells utilizing nickel-rich cathode active materials and silicon-graphite composite anodes, J. Power Sources Adv. 9 (2021) 100055, https://doi.org/10.1016/j.powera.2021.100055.

[24] F. Duffner, M. Wentker, M. Greenwood, J. Leker, Battery cost modeling: a review and directions for future research, Renew. Sustain. Energy Rev. 127 (2020) 109872, https://doi.org/10.1016/j.rser.2020.109872.

[25] F. Field, R. Kirchain, R. Roth, Process cost modeling: strategic engineering and economic evaluation of materials technologies, J. Occup. Med. 59 (2007) 21–32, https://doi.org/10.1007/s11837-007-0126-0.

[26] M. Wentker, M. Greenwood, J. Leker, A Bottom-Up approach to lithium-ion battery cost modeling with a focus on cathode active materials, Energies 12 (2019) 504, https://doi.org/10.3390/en12030504.

[27] J. Palm, Internal Fraunhofer FFB fab data, Fraunhofer FFB (2025).

[28] K. Eloot, M. van Hoey, M. Foucart, M. Azevedo, P. Bingoto, G. Hedengren, T. Vass, Global materials perspective 2024. https://www.mckinsey.com/industries/ene

rgy-and-materials/our-insights/global-materials-perspective, 2024. (Accessed 24 March 2025).
[29] SMM - Shanghai Metal Market, Spot metal prices. https://www.metal.com/, 2024. (Accessed 2 May 2024).
[30] A. Wang, Intercalation battery component price report February 2024. https://intercalationstation.substack.com/p/battery-component-price-report-march, 2024. (Accessed 30 September 2024).
[31] M. Chen, C. Zhao, Y. Li, H. Wang, K. Wang, S. Yang, Y. Gao, W. Zhang, C. Chen, T. Zhang, L. Wen, K. Dai, J. Mao, Breaking boundaries in O3-type NaNi1/3Fe1/3Mn1/3O2 cathode materials for sodium-ion batteries: an industrially scalable reheating strategy for superior electrochemical performance, J. Energy Chem. 102 (2025) 107–119, https://doi.org/10.1016/j.jechem.2024.10.038.
[32] H. Rostami, J. Valio, P. Suominen, P. Tynjälä, U. Lassi, Advancements in cathode technology, recycling strategies, and market dynamics: a comprehensive review of sodium ion batteries, Chem. Eng. J. 495 (2024) 153471, https://doi.org/10.1016/j.cej.2024.153471.
[33] C. Neef, S. Link, T. Wicke, M. Diehl, F. Degen, P. Fanz, R. Kleinert, Development Perspectives for lithium-ion Battery Cell Formats, ISI, Fraunhofer, 2022.
[34] Statista, Manufacturing Labor Costs per Hour: China, Vietnam, Mexico 2016-2020, Statista, 2017. https://www.statista.com/statistics/744071/manufacturing-labor-costs-per-hour-china-vietnam-mexico/. (Accessed 11 October 2024).
[35] Global Petrol Prices, China electricity prices, March 2024, 2024. https://www.globalpetrolprices.com/China/electricity_prices/. (Accessed 14 October 2024).
[36] IEA, Industry end-user prices for natural gas in selected countries, 2019-March 2023. https://www.iea.org/data-and-statistics/charts/industry-end-user-prices-for-natural-gas-in-selected-countries-2019-march-2023, 2023. (Accessed 14 October 2024).
[37] Turner & Townsend, ICMS international construction market survey 2024. https://assets.foleon.com/eu-central-1/de-uploads-7e3kk3/48604/cd_00120_icms_brochure_v14.3f9bcaa5ca2a.pdf, 2024. (Accessed 3 February 2025).
[38] A. Sakti, J.J. Michalek, E.R. Fuchs, J.F. Whitacre, A techno-economic analysis and optimization of Li-ion batteries for light-duty passenger vehicle electrification, J. Power Sources 273 (2015) 966–980, https://doi.org/10.1016/j.jpowsour.2014.09.078.
[39] K.W. Knehr, J.J. Kubal, S. Yoon, H. Jeon, W.J. Roh, S. Ahmed, Energy consumption of lithium-ion pouch cell manufacturing plants, J. Clean. Prod. 468 (2024) 143050, https://doi.org/10.1016/j.jclepro.2024.143050.
[40] D. Andre, S.-J. Kim, P. Lamp, S.F. Lux, F. Maglia, O. Paschos, B. Stiaszny, Future generations of cathode materials: an automotive industry perspective, J. Mater. Chem. A 3 (2015) 6709–6732, https://doi.org/10.1039/C5TA00361J.
[41] T. Hettesheimer, C. Neef, I. Inclán, S. Link, T. Schmaltz, F. Schuckert, A. Stephan, M. Stephan, A. Thielmann, L. Weymann, T. Wicke, Lithium-Ion Battery Roadmap – Industrialization Perspectives Toward 2030, Fraunhofer ISI, 2023. https://publica.fraunhofer.de/entities/publication/fc576f43-5e5f-466e-9ea1-e0f2d9e742c9. (Accessed 8 April 2025).
[42] SMM - Shanghai Metal Market, Battery-grade lithium carbonate price. https://www.metal.com/Lithium/201102250059, 2025. (Accessed 6 August 2025).
[43] SMM - Shanghai Metal Market, Battery-grade sodium carbonate price. https://www.metal.com/Sodium-ion-Battery/202404290001, 2025. (Accessed 6 August 2025).
[44] M. Mannes, Exclusive: Crisis-Hit EV Battery Champion Northvolt Struggles to Hit Production Targets, Reuters Media, 2024. (Accessed 8 April 2025).
[45] Statistisches Bundesamt - DeStatis, One hour worked cost an average of 39.50 euros in 2022. https://www.destatis.de/EN/Press/2023/04/PE23_164_624.html, 2023. (Accessed 15 May 2025).
[46] S. Orangi, N. Manjong, D.P. Clos, L. Usai, O.S. Burheim, A.H. Strømman, Historical and prospective lithium-ion battery cost trajectories from a bottom-up production modeling perspective, J. Energy Storage 76 (2024) 109800, https://doi.org/10.1016/j.est.2023.109800.
[47] X. Zhang, H.-L. Chang, C.-W. Su, M. Qin, M. Umar, Exploring the dynamic interaction between geopolitical risks and lithium prices: a time-varying analysis, Resour. Policy 90 (2024) 104840, https://doi.org/10.1016/j.resourpol.2024.104840.
[48] BloombergNEF, Lithium-Ion Battery Pack Prices See Largest Drop Since 2017, Falling to $115 per Kilowatt-Hour: Bloombergnef, BloombergNEF, 2024. https://about.bnef.com/blog/lithium-ion-battery-pack-prices-see-largest-drop-since-2017-falling-to-115-per-kilowatt-hour-bloombergnef/. (Accessed 24 March 2025).